Electronic Supporting Information for

Systematic analysis of electron energy-loss near-edge structures in Li-ion battery materials

Motofumi Saitoh,[†a] Xiang Gao,[†a] Takafumi Ogawa,[a] Yumi H. Ikuhara,[a] Shunsuke Kobayashi,[a] Craig A. J. Fisher,[a] Akihide Kuwabara[ab] and Yuichi Ikuhara[*ac]

1. Evaluation of crystallinity by X-ray diffraction (XRD)

The crystallinity of each of our samples was confirmed by XRD. Data for $LiFePO_4$,[1] $LiCoPO_4$,[2] $LiMn_2O_4$,[3] $Li_4Ti_5O_{12}$,[4] $Li_{0.33}La_{0.56}TiO_3$[5] and $Li_{0.14}La_{0.29}NbO_3$[6] have already been published elsewhere . XRD data for $LiCoO_2$, Li_2MnO_3, $LiNi_{0.5}Mn_{1.5}O_4$ and $LiNbO_3$, are shown in Fig. S1. The $LiCoO_2$ thin film sample was measured while attached to its substrate and was observed to be strongly oriented in the *c* direction. The other three samples were crushed and analysed as powders, again showing good crystallinity.

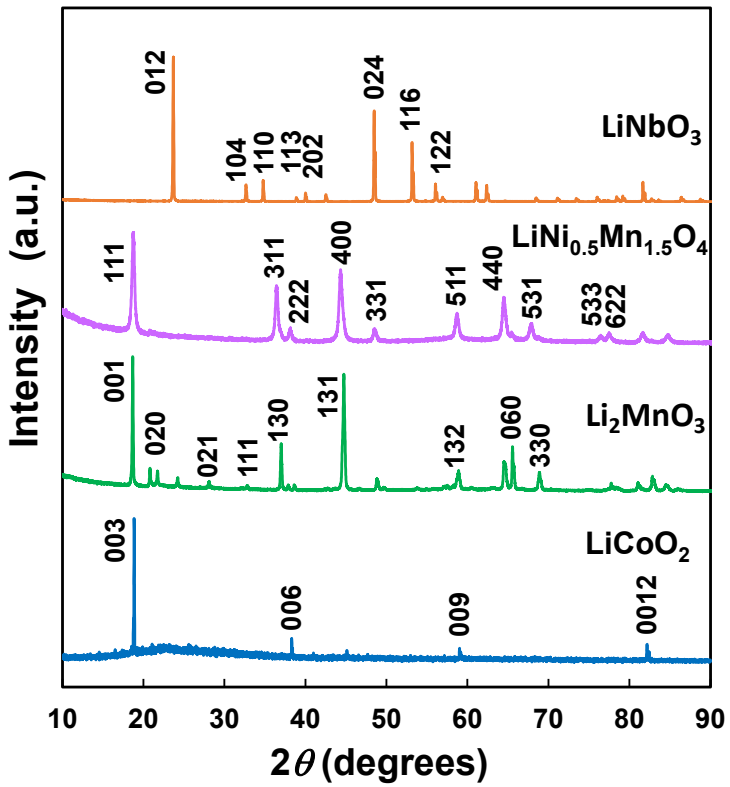

Figure S1 XRD data for $LiCoO_2$, Li_2MnO_3, $LiNi_{0.5}Mn_{1.5}O_4$ and $LiNbO_3$.

[a] *Nanostructures Research Laboratory, Japan Fine Ceramics Center, Nagoya 456-8587, Japan*
[b] *National Institute for Materials Science, Tsukuba, Ibaraki 305-0047, Japan*
[c] *Institute of Engineering Innovation, The University of Tokyo, Tokyo 113-8656, Japan*
**Corresponding Author: E-mail: ikuhara@sigma.t.u-tokyo.ac.jp*
†Authors contributed equally

2. Stability of zero-loss peak position

The accuracy of reported Li-*K* and O-*K* edges obtained by electron energy-loss spectroscopy (EELS) as well as the energy resolution, i.e., the full width half maximum (FWHM) of zero-loss peak (ZLP), is strongly affected by the stability of the electron beam. In our work, the ZLP was aligned by measuring the ZLP just before and after collecting EELS data. Figure S2 shows a typical example of the time-dependence of ZLP positions for a span of 10 minutes; the maximum deviation less than 0.1 eV and standard deviation of 0.03 eV are both small, confirming the stability of the electron microscope.

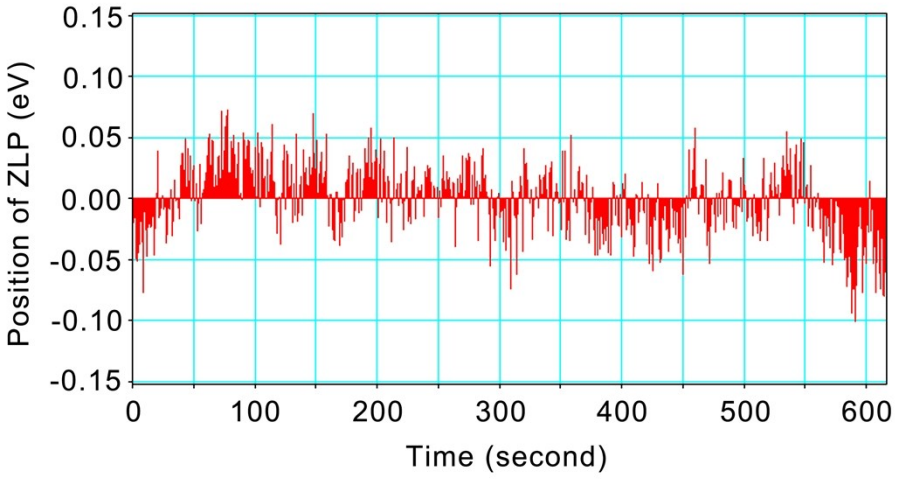

Figure S2 Time dependency of zero-loss peak position.

3. Relationship between electronic structures and O-*K* edge structures of Li-ion-battery materials

Although inclusion of the core-hole effect is necessary for quantitative comparison of simulated and experimental ELNES spectra (as described in section 3.4 of the paper), the projected densities of states (PDOSs) of compounds in the ground state can sometimes provide insights into the origins of the O-*K* ELNES peaks and why certain classes of materials have similar or dissimilar ELNES spectra. The materials examined in this study can be divided into three groups depending on the general shape of their spectra:

- Group *i* : double peaks ($Li_{0.14}La_{0.29}NbO_3$, $Li_{0.33}La_{0.56}TiO_3$, $LiNbO_3$, and $Li_4Ti_5O_{12}$)
- Group *ii* : single sharp peaks ($LiMn_{1.5}Ni_{0.5}O_4$, $LiMn_2O_4$, Li_2MnO_3, and $LiCoO_2$)
- Group *iii* : single broad beaks ($LiCoPO_4$ and $LiFePO_4$)

As mentioned in the main text, the double peaks at O-*K* edges of group *i* materials result from hybridisation of the transition metal (TM) orbitals the 2*p* orbitals of their neighbouring O ions. A schematic diagram of the PDOS of a group *i* material is shown in Fig. S3 (a). As shown in the figure, d^0 orbitals of the TM atoms are located at near the conduction band minimum (CBM) and split into t_{2g} and e_g bands as a result of their six-fold coordination environments. We note that these bands are

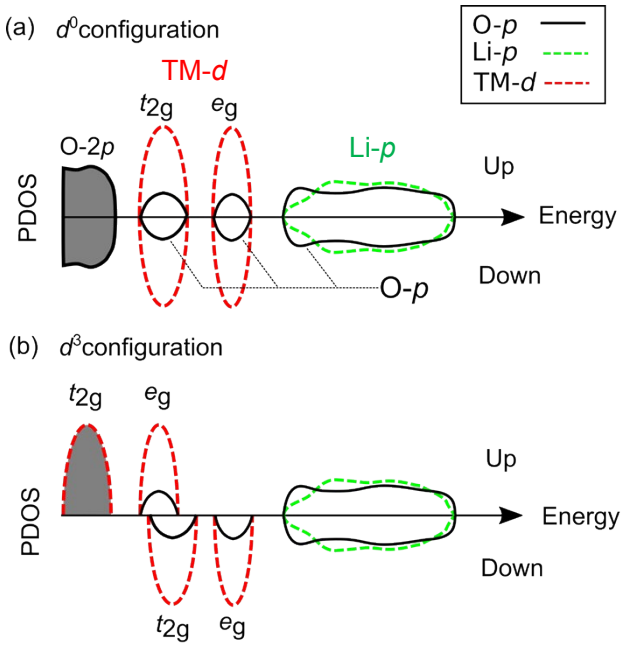

Figure S3 Schematic diagrams of PDOSs of O-*p*, Li-*p*, and TM-*d* orbitals of Li-TM-O compounds with (a) a d^0 configuration, as in group *i* materials and (b) a d^3 configuration, as in group *ii* materials containing Mn^{4+}. PDOSs of O-*p*, Li-*p* and TM-*d* orbitals are indicated by black solid, green dashed and red dashed lines, respectively. TM-*d* orbitals split into t_{2g} and e_g bands in the crystal field (six-fold coordination) formed by O atoms. The upper half and lower half of each figure represent up-spin and down-spin components, respectively. Filled areas indicate occupied states.

clearly separated from the higher energy hybridized Li-O bands. The split two unoccupied bands around the CBM include components of O orbitals into which electrons excited from O-1*s* orbital can jump, leading to the double peak in the measured O-*K* edges.

In group *ii* materials, the detection of a single sharp peak with small sub-peak in their O-*K* edges can also be explained in terms of TM-O orbital hybridisation, but in this case the TM atoms have partially occupied *d* orbitals near the CBM. A schematic diagram of the PDOS of Li_2MnO_3, which has a Mn^{4+}-d^3 configuration is shown in Fig. S3 (b). Because the up-spin component of the t_{2g} orbitals is occupied, the up-spin unoccupied e_g orbitals are shifted to lower energies relative to the down-spin components. This asymmetry in orbital energy levels results in peaks of unequal intensity in the O-*K* edges when electrons are excited from O-1*s* orbitals into the unoccupied orbitals, corresponding to the single sharp peak and sub-peak in the spectra of this group of materials.

Other compounds with partially occupied TM-*d* (and hybridized TM-O) orbitals that are well separated from orbitals of other elements are expected to produce similar O-K ELNES spectra, and thus be classified as group *ii* materials. The situation becomes more complicated when there is overlap between TM, or TM-O orbitals and orbitals of other elements in conduction band, such as occurs in olivine-type phosphates $LiFePO_4$ and $LiCoPO_4$. In such cases, the number of orbitals of different energy levels available for excited O core electrons to jump into is increased, resulting in ELNES spectra with a broad profile that are very different in shape to those of group *i* and *ii* materials, as reported in section 3.4.

References

1 A. Nakamura, S. Furutsuki, S. Nishimura, T. Tohei, Y. Sato, N. Shibata, A. Yamada and Y. Ikuhara, *Chem. Mater.*, 2014, **26**, 6178–6184.

2 Y. H. Ikuhara, X. Gao, C. A. J. Fisher, A. Kuwabara, H. Moriwake, K. Kohama, H. Iba and Y. Ikuhara, *J. Mater. Chem. A*, 2017, **5**, 9329–9338.

3 Y. H. Ikuhara, X. Gao, R. Huang, C. A. J. Fisher, A. Kuwabara, H. Moriwake and K. Kohama, *J. Phys. Chem. C*, 2014, **118**, 19540–19547.

4 A. Kumatani, S. Shiraki, Y. Takagi, T. Suzuki, T. Ohsawa, X. Gao, Y. Ikuhara and T. Hitosugi, *Jpn. J. Appl. Phys.*, 2014, **53**, 058001.

5 X. Gao, C. A. J. Fisher, T. Kimura, Y. H. Ikuhara, H. Moriwake, A. Kuwabara, H. Oki, T. Tojigamori, R. Huang and Y. Ikuhara, *Chem. Mater.*, 2013, **25**, 1607–1614.

6 X. Hu, S. Kobayashi, Y. H. Ikuhara, C. A. J. Fisher, Y. Fujiwara, K. Hoshikawa, H. Moriwake, K. Kohama, H. Iba and Y. Ikuhara, *Acta Mater.*, 2017, **123**, 167–176.